TELKOMNIKA, Vol.10, No.4, December 2012, pp. 703~714
ISSN: 1693-6930
accredited by DGHE (DIKTI), Decree No: 51/Dikti/Kep/2010

Fluctuations Mitigation of Variable Speed Wind Turbine through Optimized Centralized Controller

Ali Mohammadi*, Sajjad Farajianpour, Saeed Tavakoli, and S. Masoud Barakati
Faculty of Electrical and Computer Engineering, University of Sistan and Baluchestan, Iran
e-mail: a.mohammadi@mail.usb.ac.ir*, s.farajian@mail.usb.ac.ir, tavakoli@ece.usb.ac.ir, smbaraka@ece.usb.ac.ir

Abstrak

Suatu sistem konversi energi angin (WECS) yang mengandung jenis pembangkitan tenaga angin yang dapat diatur dan terhubung dangan jala jala sangat diperlukan untuk dikendalikan. Dalam tulisan ini setiap komponen model WECS secara sistematik disajikan dan diintegrasikan serta divalidasi. Sifat alamimiah dari WECS yang non linier dan struktur sistem yang kompleks yang diasumsikan sebagai sistem yang memiliki masukan jamak dan keluaran jamak (MIMO), telah membuat sistem ini sulit untuk dibuat strategi kendalinya. Untuk menyederhanakan rancangan kendali, suatu pengendali terpusat yang bersesuaian dengan model sistematik tadi telah diterapkan. Untuk menambah unjuk kerja pengendali terpusat, suatu algoritma generik untu optimasi disertakan. Hasil simulasi menunjukkan efektitifas strategi kendali yang diusulkan untuk mengatasi perpindahan fluktuasi.

***Kata kunci**: algoritma genetik (GA), masukan jamak dan keluaran jamak (MIMO), migitasi fkuktuasi, pengendali optimum terpusat, sistem konversi energi angina (WECS)*

Abstract

A wind energy conversion system (WECS) including a variable wind turbine in grid-connected mode is considered to control. In this paper, each component of WECS model is systematically presented and then the integrated overall model is validated.Regarding to nonlinear nature of WECS and the complex system structure as multiple-input multiple-output (MIMO), it is difficult to find a proper control strategy. To simplify the control design, a centralized controller, which is compatible with systematic modelling, is employed. In addition, to enhance the centralized controller performance, an optimization based on genetic algorithm (GA) is accomplished. Simulation results demonstate the effectivesness of the proposed control startegy to mitigation fluctuations.

***Keywords**: fluctuations mitigation, genetic algorithm (GA), optimized centralized controller, multiple-input multiple-output (MIMO), wind energy conversion system (WECS)*

1. Introduction

Wind energy importance from standpoint of economical, environmental, and accessibility aspects attracts much attention to itself rather than other energy types [1]. In spite of its advantages, it contains operation problems as intermittent capture results in low efficiency, poor naturally controllability and predictability [1]. Hence, wind energy conversion system (WECS) control is undeniably considered as a problem to its operation. Works done in this issue differs from standpoint of control methods, the controlled variables, and the system requirements to meet.

Most literatures focus on control methods applicable in electrical drives. In [2] , a vector control (VC) is used to fix voltage amplitude and frequency for different loading conditions. In [3], a direct power control (DPC) based on sliding mode control (SMC) is supposed to be an alternative to conventional (lookup table) LUT DPC and classic VC. Couple of papers work on hybrid strategies combined of pure control with proposed approaches. In [4], a proportional-derivative (PD) controller and a loop control is employed in the aim to capture maximum tracking using a look up table interpolation containing curves family containing dc voltages versus optimal power for different wind speeds. Some literatures are emphasized on methodologies based on control principles systematically implementable. Abedini et al. [5] provided output power and voltage control under wind speed and load demand variations, large transients and finally islanding events using four decentralized proportional–integral (PI)

Received April 18, 2012; Revised September 5, 2012; Accepted September 13, 2012

controllers with the capability to dispatch power among generator, grid and the battery . In [6], control design are established with small signal analysis to take account into the damping and stability parameters convertible into multi-objective optimization based on differential evolution (DE) to obtain optimal results. Another method is based on nonlinear robust controller to meet both requirements on the network and considering the characteristics system [7].

In previous works, control strategies are accordance with predefined objective. In this study, an attempt is made to employ a simple and easily-implementing strategy in optimized centralized manner to achieve enhanced properties instead of sophisticated methodologies.

This paper is organized as follows: Each compartment of WECS modelling including drive train, power electronic converter, and the generator dynamically are independently presented and the overall equations are integrated and validated through simulation. In section2.8centralized controller structure applied to WECS is explained and finally with respect to contrlled variables, control design is accomplished using GA. Finally, last section is dedicated to conclusions.

2. Research Method

Generally, to design a realistic controller systematically, it necessitates having the model represented in state space equations. Thus, there has been an attempt to model each component of WECS independently and obtain the overall model in valid manner. Wind turbine is the major component of a WECS to convert wind energy into aerodynamic. The drive train is necessary to translate aerodynamic into mechanical energy. The generator is about to produce electrical power, being WECS heart. There should be a mechanism to smooth the fluctuating power corresponding to different wind speed which is applicable through power conditioner. Representation of these components are organized as follows.

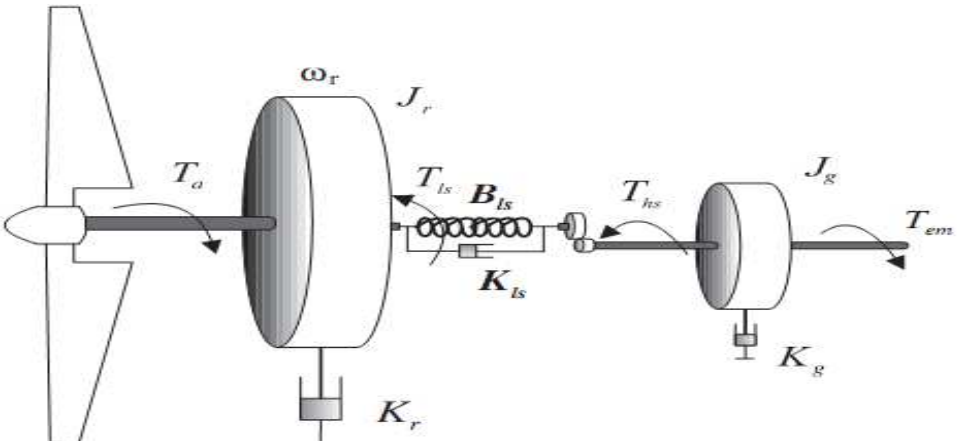

Figure 1. Drive train two-mass model

2.1. Drive Train

Drive train model should be represented so that it considers adequate description and avoids extra computation especially in large power system. The most common models are two-mass and six-mass [8]-[10]. Latter includes high order, thus it is not appropriate for large power system. As two-mass model features adequate accuracy and decreasingly computation, it is the best choice to consider. In this model, all masses are lumped at low and high speed shaft. The inertia of the low speed shaft comes mainly from the blades and the inertia of the high speed shaft from the generator (Figure 1). After writing Newton law for low-speed and high-speed shaft and taking into account the self damping of turbine and generator, mutual damping and the system stiffness, state space representation is obtained as follows:

$$\dot{\omega}_t = \frac{1}{J_t}\left(T_t - T_s - D_t\omega_t\right) \quad (1)$$

$$\dot{\omega}_g = \frac{1}{J_g}\left(-T_e + \frac{T_s}{n} - D_g\omega_g \right) \quad (2)$$

$$\dot{T}_s = K_s\left(\omega_t - \frac{\omega_g}{n} \right) + D_s\left(\dot{\omega}_t - \frac{\dot{\omega}_g}{n} \right) \quad (3)$$

where, ω_t , ω_g , T_s angular speed of the turbine and the generator and shaft torque, T_t aerodynamic torque, T_e the generator electromagnetic torque, J_t , J_g turbine and the generator inertia, D_t, D_g self damping of the turbine and the generator, K_s, D_s stiffness and mutual damping and n, the gearbox ratio.

To make modelling more realistic, it is necessary to incorporate aerodynamic torque and electromagnetic torque in the following subsections.

2.2. Aerodynamic Torque

One can model this torque through dividing power captured from the wind by the rotational turbine speed [1] as:

$$T_t = \frac{1}{2}\rho_{air} A_r \frac{v_w{}^3 c_p(\beta, \lambda)}{\omega_t} \quad (4)$$

where, air density, A_r the rotor area swept by the blades, v_w effective wind speed met by the rotor and power coefficient, in a variable speed turbine, being a function of the tip speed ratio and pitch angle. Hence, wind speed and pitch angle models are needy to be represented.

2.3. Wind Speed

One model to consider, is presented as superposition of four component including the average value, ramp component, gust component and noise component [11] . With respect to the turbulent described in the frequency domain while the others in time, a conflict encountered during the calculation. Another model which overcomes this problem is composed of two components [12]: low frequency and high frequency. This model is given by sum of mean wind speed and a random process in sinusoidal term as:

$$v_w = A_0 + \sum_{i=1}^{N} A_i \cos(\omega_i t + \varphi_i) \quad (5)$$

where , A_0 denotes wind speed mean calculated on a time horizon usually 10 minutes, A_i the amplitude of i-th harmonic in terms of the discrete angular frequency and the corresponding power spectral density obtained by (6) and φ_i is generated in a uniform random distribution on interval $[-\pi,\pi]$.

$$A_i = \frac{2}{\pi}\sqrt{\frac{1}{2}\left(s_{vv}(\omega_{i+1}) + s_{vv}(\omega_i)\right).(\omega_{i+1} - \omega_i)} \quad (6)$$

Spectral density in (6) is commonly determined based on the Van der Hoven, Von Karman, and Kaimal models. Vander Hoven model has poor representation on low frequency component due to independency mean wind speed. Hence, the Kaimal and Karman spectral densities are preferred. Though Kaimal's spectrum have better correspondence at turbulence presence [13], Karman's spectrum present more realistic performance in wind tunnels [14]. So in this study, Karman spectrum stated in terms of the turbulence length (L), standard deviation (σ) and mean wind speed (V_{WM}) is specified as follows:

$$S(\omega)=\frac{0.475\sigma^2\frac{L}{v_m}}{\left[1+\left(\frac{\omega L}{v_m}\right)^2\right]^{\frac{5}{6}}}. \quad (7)$$

Considering wind speed passing through the blades, high frequency damping and shadow effect are about to be modelled. High frequency damping can be approximately represented as a low pass filter [15].

$$H(s)=\frac{1}{\tau s+1} \quad (8)$$

Shadow effect results in periodic torque pulsation caused by passing any blade across the tower. This phenomenon is modelled by adding a sinusoidal periodic torque at N times mechanical speed where N is blades number [16]. Figure 2 demonstartes the wind speed in time domain, considering the effective model above. The Wind tunnel parameteres are available in Appendix I.

2.4. Pitch Angle Model

To track desired pitch angle, a control system is needed. This task is accomplished via the hydraulic actuator. Pitch angle dynamic is represented as a first-order constrained by the amplitude and derivative of the output pitch (Figure 2). With the assumption to working in linear region, state space to pitch angle is yielded as Equation (9) where β_{ref} denotes desired pitch angle and τ_β time constant. Practically, β ranges from -2^o to 3^o and varies at a maximum rate of $\pm 10\ o/s$ [17] .

$$\dot{\beta}=\frac{1}{\tau_\beta}(\beta_{ref}-\beta) \quad (9)$$

2.5. Generator Model

To consider the electromagnetic torque meaningfully, it is necessary to develop all dynamics associated to the generator. In this study, squirrel cage induction generator (IG) is employed. Due to simplicity, machine equations are described at dqo reference frame.

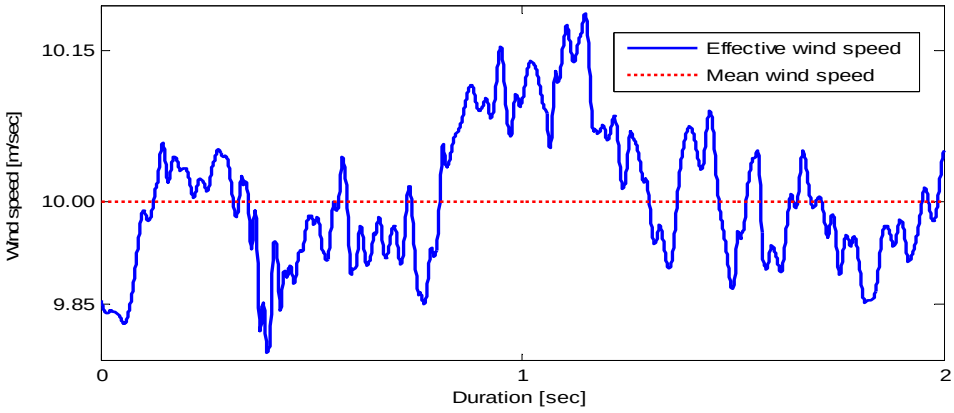

Figure 2. Wind speed simulation

Hence, it is essential to transform *abc* coordinates into synchronously rotating dqo reference frame through Park transformation as follows [18]:

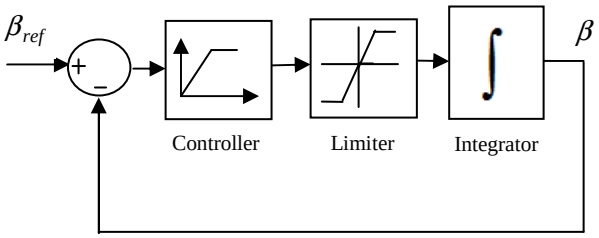

Figure 3. Pitch angle block digram

$$\begin{bmatrix} f_q \\ f_d \end{bmatrix} = \begin{bmatrix} cos(\theta) & cos(\theta - \frac{2\pi}{3}) & cos(\theta + \frac{2\pi}{3}) \\ sin(\theta) & sin(\theta - \frac{2\pi}{3}) & sin(\theta + \frac{2\pi}{3}) \end{bmatrix} \begin{bmatrix} f_a \\ f_b \\ f_c \end{bmatrix} \tag{10}$$

where, $\theta = \int \omega dt$, ω set to stator electrical speed at synchronously rotating reference frame. Further, IG state equations in terms of flux linkage is represented as [18]:

$$\dot{\psi}_{qs} = -\omega_b \frac{r_s X_{rr}}{D} \psi_{qs} - \omega \psi_{ds} + \omega_b \frac{r_s X_M}{D} \psi_{qr} + \omega_b v_{qs} \tag{11}$$

$$\dot{\psi}_{ds} = \omega \psi_{qs} - \omega_b \frac{r_s X_{rr}}{D} \psi_{qs} + \omega_b \frac{r_s X_M}{D} \psi_{dr} + \omega_b v_{ds} \tag{12}$$

$$\dot{\psi}_{qr} = \omega_b \frac{r_r X_M}{D} \psi_{qs} - \omega_b \frac{r_r X_{ss}}{D} \psi_{qr} - (\omega - \omega_r) \psi_{dr} \tag{13}$$

$$\dot{\psi}_{dr} = \omega_b \frac{r_r X_M}{D} \psi_{ds} + (\omega - \omega_r) \psi_{qr} - \omega \frac{r_r X_{ss}}{D} \psi_{dr} \tag{14}$$

where, ψ_{qs} , ψ_{qs} q-axis and d-axis stator flux linkages , ψ_{qr} , ψ_{dr} q-axis and d-axis rotor flux linkages, $X_{ss} = X_{ls} + X_M$, $X_{rr} = X_{lr} + X_M$, $D = X_{ss} X_{rr} - X_M{}^2$, r_s, r_r stator and rotor resistances, X_{ls}, X_{lr} stator and rotor leakage reactances and X_M magnetization reactance, ω , ω_r , ω_b stator electrical angular speed, rotor electrical angular speed and base angular speed, v_{qs} , v_{ds} , q-axis and d-axis stator voltages. Finally, the developed electromagnetic torque is computed in terms of the flux linkages and poles number (*p*) as:

$$T_e = \frac{3}{2} \frac{p}{2} \frac{X_M}{D \omega_b} (\psi_{qs} \psi_{dr} - \psi_{ds} \psi_{qr}) \tag{15}$$

Alternatively, IG currents are calculated in terms of flux linkages in the following matrix.

$$\begin{bmatrix} i_{qs} \\ i_{ds} \\ i_{qr} \\ i_{dr} \end{bmatrix} = \frac{1}{D} \begin{bmatrix} X_{rr} & 0 & -X_M & 0 \\ 0 & X_{rr} & 0 & -X_M \\ -X_M & 0 & X_{ss} & 0 \\ 0 & -X_M & 0 & X_{ss} \end{bmatrix} \begin{bmatrix} \Psi_{qs} \\ \Psi_{ds} \\ \Psi_{qr} \\ \Psi_{dr} \end{bmatrix} \tag{16}$$

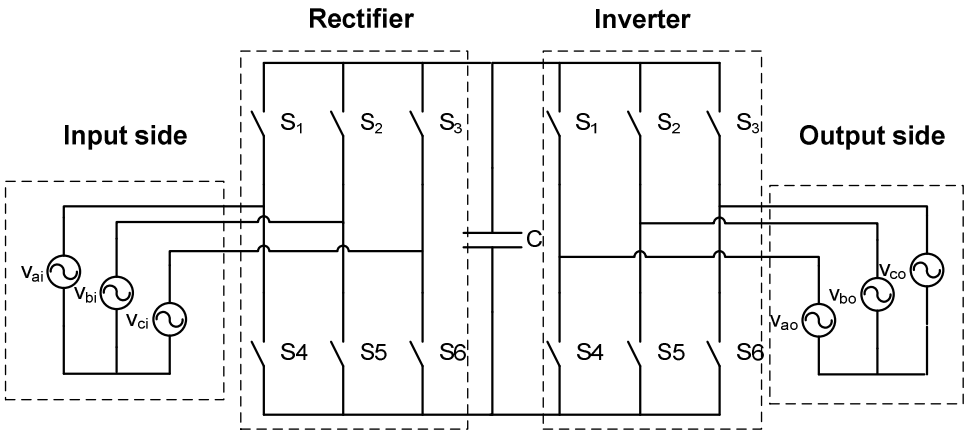

Figure 4. VSC-VSC topology

2.6. Converter Model

A converter plays a prominent role in power conditioning. Among various structures and topologies, back-back VSCc in full-rated scheme is employed (Figure 4) in light of flexibility it features [19]. To finalize modelling, it is adequate to develop v_{qs} and v_{ds} through dynamics imposed by the converter. For simplification of control design, the converter model should be accomplished in fundamental frequency neglecting switching dynamics, and in *dqo* reference frame to be compatible with IG model. Model presented in [20] has above both properties where linear equations with constant frequencies assumption are represented in terms of input and output currents and capacitor voltage as follows:

$$\dot{i}_{qi} = \frac{1}{L_i}\left[-R_i i_{qi} - L_i \omega_i i_{di} + v_{qi} - v_{qin}\right] \quad (16)$$

$$\dot{i}_{qi} = \frac{1}{L_i}\left[-R_i i_{qi} - L_i \omega_i i_{di} + v_{qi} - v_{qin}\right] \quad (17)$$

$$\dot{i}_{di} = \frac{1}{L_i}\left[-R_i i_{di} + L_i \omega_i i_{qi} + v_{di} - v_{din}\right] \quad (18)$$

$$\dot{i}_{qo} = \frac{1}{L_o}\left[-R_o i_{qo} - L_o \omega_o i_{do} - v_{qo} + v_{qou}\right] \quad (19)$$

$$\dot{i}_{do} = \frac{1}{L_o}\left[-R_o i_{do} + L_o \omega_o i_{qo} - v_{do} + v_{dou}\right] \quad (20)$$

$$\dot{v}_d = \frac{1}{C}\frac{3}{4}\left[i_{qin} + i_{din} - i_{qou} - i_{dou}\right] \quad (21)$$

where, i_{qi},, i_{di} are *q*-axis and *d*-axis currents coming from input, i_{qo}, i_{do} *q*-axis and *d*-axis output currents going to output, v_d capacitor voltage, and

$$i_{qin} = A_{mi} i_{qi} sin(\alpha_{mi} - \alpha_i),\ i_{din} = A_{mi} i_{di} cos(\alpha_{mi} - \alpha_i),\ i_{qou} = A_{mo} i_{qo} sin(\alpha_{mo} - \alpha_i),$$
$$i_{dou} = A_{mo} i_{do} cos(\alpha_{mo} - \alpha_o),\ v_{qin} = 0.5 v_d sin(\alpha_{mi} - \alpha_i)\ v_{din} = 0.5 v_d cos(\alpha_{mi} - \alpha_i),$$

$v_{dou} = 0.5 v_d sin(\alpha_{mo} - \alpha_o)$ $v_{dou} = 0.5 v_d cos(\alpha_{mo} - \alpha_o)$, $v_{qi} = v_i sin(\alpha_i)$, $v_{di} = v_i cos(\alpha_i)$, $v_{qo} = v_o sin(\alpha_o)$, $v_{do} = v_o cos(\alpha_o)$, v_i, v_o amplitude of the input and output voltage sources, R_i, L_i input resistance and inductance, R_o, L_o output resistance and inductance, C, capacitor capacity of dc-link between two converters, ω_i, ω_o input and output electrical rotational speeds, α_i, α_o phase angle of the input and output voltages, A_{mi}, α_{mi}, A_{mo}, α_{mo} amplitude and phase modulation indices of input and output converters. In this model, pulse width modulation (PWM) technique from transforming switching reference frame into *dqo* is converted to modulation indices as converter inputs. Note that amplitude and phase modulations are definably on interval [0 1] and [-π, π], respectively.

2.7. Overall Model of WECS

To achieve the overall modelling, it is essential to integrate the shared-variable equations and eliminate equivalent variables and form the state space representation as follows:

$$\dot{\psi}_{qs} = a_{1,0}\left[\omega_b{}^2 L_o \frac{r_r X_{M^2}}{D^2} - \omega_b \frac{(R_o + r_s)X_{rr}}{D}\right]\psi_{qs} - a_{1,0}\left[\omega_b \frac{L_o \omega X_{rr}}{D}\psi_{ds} + \omega\right]\psi_{ds} +$$
$$a_{1,0}\left[\omega_b \frac{(R_o + r_s)X_M}{D} - \omega_b{}^2 L_o \frac{r_r X_{ss} X_M}{D^2}\right]\psi_{qr} + a_{1,0}\omega_b \frac{L_o \omega_r X_M}{D}\psi_{dr} + a_{1,0}\omega_b v_{qou},$$
$$\dot{\psi}_{ds} = a_{1,0}\left[\omega_b \frac{L_o \omega X_{rr}}{D}\psi_{ds} + \omega\right]\psi_{qs} + a_{1,0}\left[\omega_b{}^2 L_o \frac{r_r X_{M^2}}{D^2} - \omega_b \frac{(R_o + r_s)X_{rr}}{D}\right]\psi_{ds}$$
$$- a_{1,0}\omega_b \frac{L_o \omega_r X_M}{D}\psi_{qr} + a_{1,0}\left[\omega_b \frac{(R_o + r_s)X_M}{D} - \omega_b{}^2 L_o \frac{r_r X_{ss} X_M}{D^2}\right]\psi_{dr} + a_{1,0}\omega_b v_{dou},$$
$$\dot{\psi}_{qr} = \omega_b \frac{r_r X_M}{D}\psi_{qs} - \omega_b \frac{r_r X_{ss}}{D}\psi_{qr} - (\omega - \omega_r)\psi_{dr},$$
$$\dot{\psi}_{dr} = \omega_b \frac{r_r X_M}{D}\psi_{ds} + (\omega - \omega_r)\psi_{qr} - \omega \frac{r_r X_{ss}}{D}\psi_{dr},$$
$$\dot{i}_{qg} = \frac{1}{L_i}\left[-R_i i_{qg} - L_i \omega_i i_{dg} + v_{qg} - v_{qgn}\right],$$
$$\dot{i}_{dg} = \frac{1}{L_i}\left[-R_i i_{dg} + L_i \omega_i i_{qg} + v_{dg} - v_{dgn}\right],$$
$$\dot{v}_d = -a_{7,0}\frac{X_{rr}}{D}A_{mo} sin(\alpha_{mo} - \alpha_{oi})\psi_{qs} - a_{7,0}\frac{X_{rr}}{D}A_{mo} cos(\alpha_{mo} - \alpha_o)\psi_{ds} + a_{7,0}\frac{X_M}{D}A_{mo} sin(\alpha_{mo} - \alpha_o)\psi_{qr}$$
$$+ a_{7,0}\frac{X_M}{D}A_{mo} cos(\alpha_{mo} - \alpha_o)\psi_{dr} + a_{7,0}A_{mi} sin(\alpha_{mi} - \alpha_i)i_{qg} + a_{7,0}A_{mi} sinos(\alpha_{mi} - \alpha_i)i_{dg},$$
$$\dot{\omega}_t = -\frac{D_t}{J_t}\omega_t - \frac{1}{J_t}T_s + \frac{1}{J_t}T_t,$$
$$\dot{\omega}_r = -\frac{D_t}{J_t}\omega_r + \frac{1}{nJ_g}T_s + \frac{1}{J_g}T_e,$$
$$\dot{T}_s = \left[K_s - \frac{D_s D_t}{J_t}\right]\omega_t - \frac{1}{n}\left(K_s - \frac{D_s D_g}{J_g}\right)\omega_r - D_s\left(\frac{1}{J_t} + \frac{1}{n^2 J_g}\right)T_s + \frac{D_s}{J_t}T_t + \frac{D_s}{nJ_g}T_e,$$
$$\dot{\beta} = -\frac{1}{\tau_\beta}\beta + \frac{1}{\tau_\beta}\beta_{ref}. \quad (22)$$

where subscript *g* denotes grid variables replaced for input variable subscript *i* and

$$a_{1,0} = \left[1 + \omega_b \frac{L_o X_{rr}}{D}\right]^{-1},\ a_{7,0} = \frac{0.75}{C}.$$

To make sure of valid modelling, the simulated WECS is proposed to inject active and

reactive power conveniently in an open loop manner.

2.8. Control Design

For the MIMO system under study, a centralised controller based on PID in cascaded scheme (Figure 5) is employed, due to its easy implementation and common application in industry. Variables to problem design are injected reactive and active power into the grid, q-axis current and dc-link voltage. Compensator dimension with respect to manipulated and controlled variables is assigned as 4×4. As WECS under study is extremely nonlinear, PID coefficients assignment is a challenging task to meet the best performance. In this study, there has been an attempt to employ the approach including simple implementation using GA rather than methods based on control principle as pole placement. As a PID includes K_p, P_i, T_d coefficients, totally, there are 16 optimal parameters. The aim to control is to have the most optimal performance in reference tracking. Among different performance indices common in control principle, Integral Abs Error (IAE) is preferred to others due to involving reasonable view of error reduction. This multi-objective problem is easily convertible into single objective through weighted-sum method [21] as follows:

$$min\ F(k) = \sum_{i=1}^{4} C_i IAE_i \tag{23}$$

where C_i, IAE_i are the weight and IAE asscociated to the i^{th} controlled variable.

3. Results and Analysis

In this section, each component is indepedency simulated and after assurrance of their validation, them all integrated to represent a WECS and then controlled through the proposed optimized strategy. System under syudy is composed of variable wind turbine driven by IG conditioning with Full–rated converter in grid-connected mode. All parameteres regarding to the simulations are given in Appendix I.

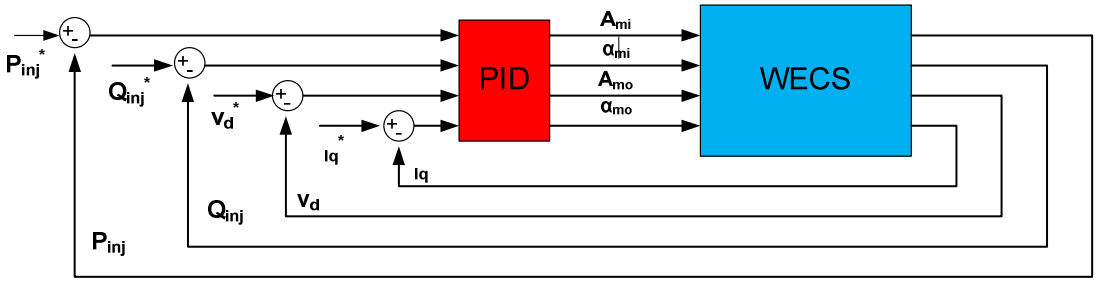

Figure 5. Controller configuration

Using Equations (11)-(14), a simulation is started by running IG initially in motoring mode at t=0 sec and then wind turbine applied into generator at t=2 sec. During the starting, all states after a transient behavior, reached steady state values and speed machine was increased till close to synchronous speed (Figure 6). T_e also was fixed to zero after meeting a maximum value, presenting natural behavior of IG. After switching in generative mode integrated into wind turbine, machine performed as so to inject power into the grid, being evident from negative final value of *Te*, which is the sign of machine working generatively.

To check the model validation of the converter, a simulation is performed based on state equations (16)-(19). PWM signal parameters are determined according to table I. Regarding to this model having negative-real part eigenvalues, it behaves stably. Results verified this with a n overshoot implying eigen-values including dominant imaginary parts (Figure 7).

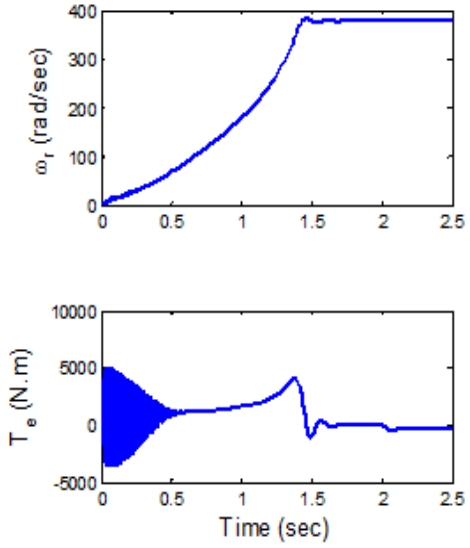

Figure 6. IG validation simulation

Table 1. Modulation indices during the simulation

A_{mi}	α_{mi}	A_{mo}	α_{mo}	α_i	α_o
0.8	-43 [deg]	0.92	21[deg]	0 [deg]	0 [deg]

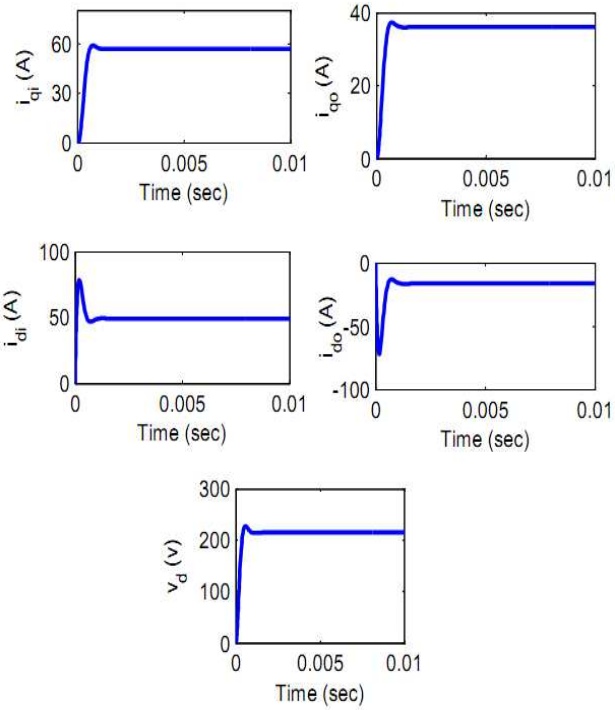

Figure 7. Converter reponses to PWM signals

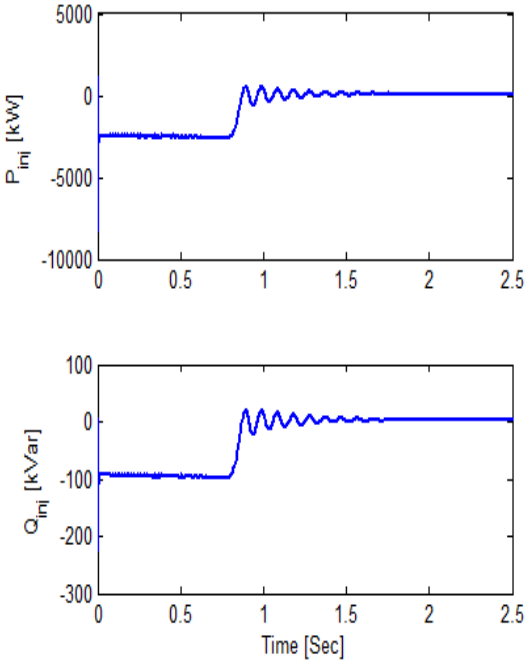

Figure 8. The Overal WECS behavior to manual input

Table 3. GA parameters

Parameters	Value
Population	20
Stop criteria	50
Fitness scaling	Rank
Selection function	Roulette
Crossover function	Heuristic
Crossover rate	0.6
Mutation function	Uniform
Mutation rate	0.03

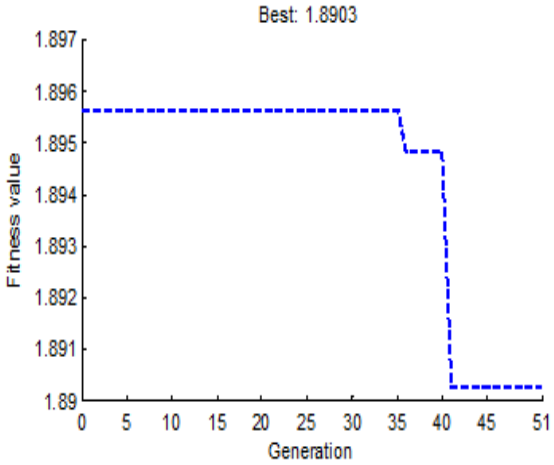

Figure 9. Best fitness during generations

Table 2. Reference values for converter simulation

i_q^*	v_d^*	P_{inj}^*	Q_{inj}^*
0	8.3 [kV]	36 [kW]	0 [kVar]

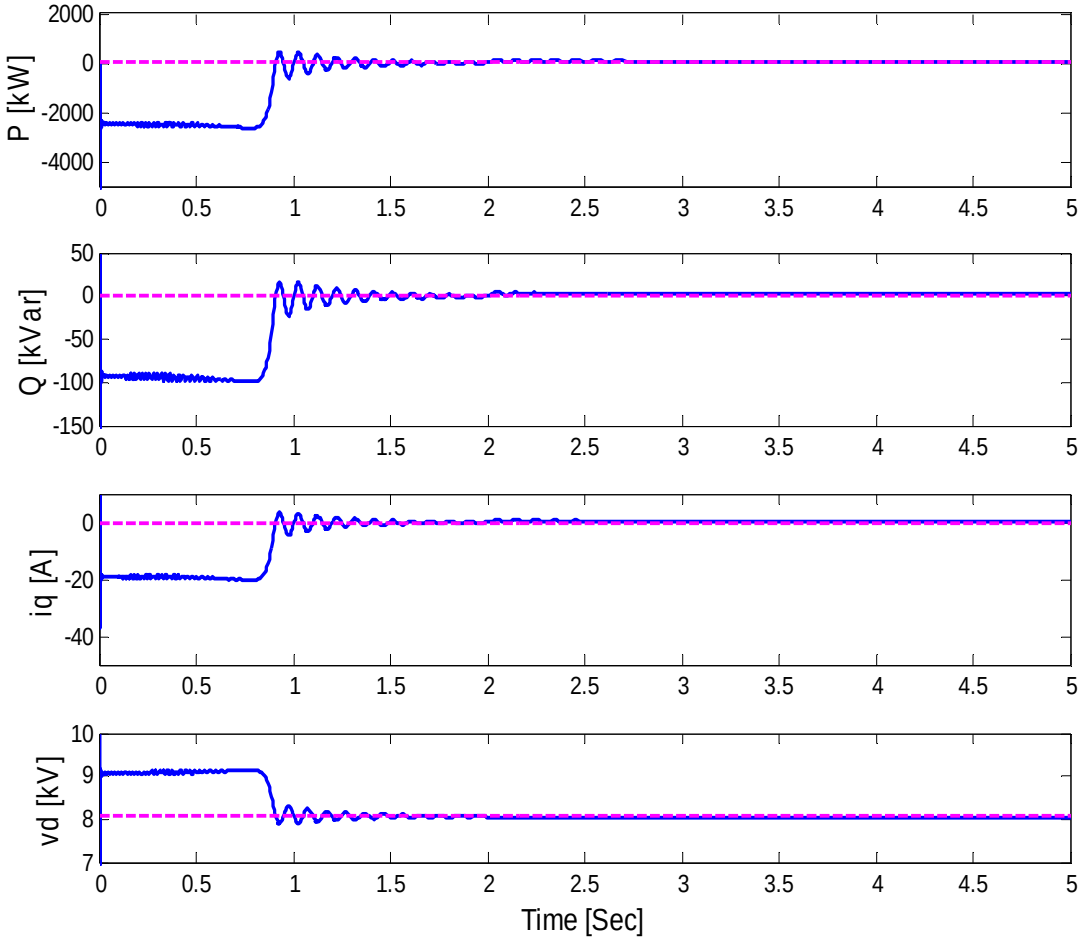

Figure 10. Controlled variables vs. desired through optimized controller

Furtehrmore, the capacitor has been a reactive interface to help active and reactive power transfer, maintaining its voltage.

Sunsequently, afterward all models were validated, the main task to check the overall model, obtained by equations (22), is accomplished. To operate IG generatively, it is required to work initially as a motor to absorb needy active and reactive power to provide its magnetizing current. At t=2 sec, it is switched into generative mode with input, transiting some damped oscillations, it begins to inject active and reactive power corresponding to control signal applied (Figure 8), hence WECS model is validated.

Centrailised controller optimized via GA is embedded over WECS to track as accurate responses as possible in comparison to desired. Reference values during the simulation are shown in Table II.

GA was performed to solve objective (23) including parameters as tabl III.GA managed to obtain optimal coefficients in 51 generations results in objective (23) to 1.8994 (Figure 9). Simulation results to reponses show successful performance in flutuation mitigation resulted from GA based on PID in error reduction (Figure 10).

4. Conclusion

A grid-connected IG-driven WECS equipped with FRC converter is dynamically modelled at fundamental frequency. Centralized controller based on PID due to its dramatic application was embedded over WECS in cascade structure. PID performance was optimally augmented through GA so that, considering multiple controlled variables and multi-objective system was convertible into single-objective via weighted-sum method. Simulation results verified proper performance of the proposed strategy. Future work will contain incorporating a system storage and employing the decentralized controller to power quality problems at variable wind speed and load demands. In addition investigating of system robustness especially in uncertainty condition will be performed.

Appendix I

Table 4. WECS parameters during the simulations

Induction generator	Drive train	Converter
500 [*hp*], 2.3 [*KV*], 1773 [*rpm*]	J_t=100 [$kg.m^2$]	R_i=1,R_o=1 [Ω]
$r_s = 0.262, r_r = 0.187$ [Ω]	K_S=2×10^6 [*Nm/rad*]	L_i=0.1,L_o=0.1 [*mH*]
X_{ls} =1.206, X_{ls} =1.206, X_M =54.02 [Ω]	D_S=5×10^3, D_t=D_g=0 [*Nm/rad/sec*]	v_i=110,v_o=110 [*V*] v_g=4 [*kV*]
J_g=11.06 [kg.m^2], P=4 [*poles*]	n=25	$\omega_i = \omega_o = 2\pi \times 60$ [*rad/sec*]

References

[1] Mathew S. Wind Energy Fundamentals Resource Analysis and Economics. Springer-Verlag Berlin Heidelberg. 2006.
[2] Haque M. E., Negnevitsky M. and Muttaqi K. M. A Novel Control Strategy for a Variable-Speed Wind Turbine With a Permanent-Magnet Synchronous Generator. *IEEE Trans. on Industry Applications*. 2010; 46(1).
[3] Hu J., Nian H., Hu B., He Y. and Zhu Z. Q. Direct Active and Reactive Power Regulation of DFIG Using Sliding-Mode Control Approach. *IEEE Trans. on Energy Conversion*. 2010; 25(4).
[4] Tan K. and Islam S. Optimum Control Strategies in Energy Conversion of PMSG Wind Turbine System Without Mechanical Sensors. *IEEE Trans. Energy Conversion*. 2004; 19(2).
[5] Abedini A. and Nikkhajoei H. Dynamic Model and Control of a Wind-turbine Generator with Energy Storage. *IET Renew. Power Gener.* 2011; 5(1): 67–78.
[6] Yang L., Yang G.Y., Xu Z., Dong Z.Y., Wong K.P. and Ma X. Optimal Controller Design of a Doubly-fed Induction Generator Wind Turbine System for Small Signal Stability Enhancement. *IET Gener., Transm. & Dist*. 2010; 4(5): 579-597.
[7] Hu Ji., Nian H., Hu B., He Y. and Zhu Z.Q. Direct Active and Reactive Power Regulation of DFIG using Sliding-mode Control Approach. *IEEE Trans. Energy Convers*. 2010; 25(4): 1028-1039.
[8] Akhmatov V. Variable-speed Wind Turbines with Doubly-fed Induction Generators. Part I. *Modelling in Dynamic Simulation Tools, Wind Engineering*. 2002; 26(2): 85–108.
[9] Ackermann T. Wind Power in Power Systems. John Wiley & Sons, Ltd. Chichester. 2005: 536–546.
[10] Papathanassiou S. A. and Papadopoulos M. P. Mechanical Stress in Fixed Speed Wind Turbines due to Network Disturbance. *IEEE Transactions on Energy Conversion*. 16(4): 361–363.
[11] Anderson P. M. and Bose A. Stability Simulation of Wind Turbine Systems. *Power Apparatus and Systems.* 1983; 102(12): 3791-3795.
[12] Nichita C., Luca D., Dakyo B. and Ceanga E. Large Band Simulation of the Wind Speed for Real Time Eind Turbine Simulators. *IEEE Trans. on Energy Conversion*. 2002; 17(4): 523 – 529.
[13] Burton T., Sharpe D., Jenkins N. and Bossanyi E. Wind Wnergy Handbook. John Wiley & Sons, New-York. 2001.
[14] Munteanu. I., Bratcu A. I., Cutululis N. A, Ceanga E. Optimal Control of Wind Energy Systems: Towards a Global Approach. *Advances in Industrial Control*. Springer–Verlag London. 2008.
[15] Wu J., Dong P., Yang J.M. and Chen Y.R. *A Novel Model of Wind Energy Conversion System*. in Proc. DRPT2004. IEEE International Conf. on Electric Utility Deregulation and Power Technologies. April 2000.
[16] Slootweg J.G., Polinder H., and Kling W.L. Representing Wind Turbine Electrical Generating Systems in Fundamental Frequency Simulations. *IEEE Trans. on Energy Conversion*. 2003; 18(4): 516-524.
[17] Bianchi F. D., Battista H. D. and Mantz R. J. Wind Turbine Control Systems. *Advances in Industrial Control.*Springer–Verlag London. 2007.

[18] Krause P. C., Wasynczuk O. and Sudhoff S. D. Analysis of Electric Machinery. *IEEE Press*. 1994.
[19] Anaya-Lara O., Jenkins N., Ekanayake J., Cartwright P. and Hughes M. Wind Energy Generation Modelling and Control. John Wiley & Sons. 2009.
[20] Nikkhajoei, H., Iravani, R. Dynamic Model and Control of AC-DC-AC Voltage-Sourced Converter System for Distributed Resources. *IEEE Trans. Power Deliv*. 2007: 22(2): 1169–1178.
[21] Deb K. Multi-objective Optimization using Evolutionary Algorithms. Wiley, New York. 2001.